Human Brain Mapping

WILEY

RESEARCH ARTICLE OPEN ACCESS

Hidden Rhythms of a Developing Brain: Multimetric rs-fMRI Insights Into Typical Youth Maturation

Merida Galilea Tapia-Medina[1,2,3] | Raquel Cosío-Guirado[1,2,3] | Maribel Peró-Cebollero[1,2,3] | Cristina Cañete-Massé[1] | Erwin Rogelio Villuendas-González[4] | Joan Guàrdia-Olmos[1,2,3]

[1]Department of Social Psychology and Quantitative Psychology, University of Barcelona, Barcelona, Spain | [2]Institute of Complex Systems, University of Barcelona, Barcelona, Spain | [3]Institute of Neuroscience, University of Barcelona, Barcelona, Spain | [4]Faculty of Psychology, Universidad Michoacana de San Nicolás de Hidalgo, Morelia, México

Correspondence: Merida Galilea Tapia-Medina (galilea.tapia@ub.edu)

Received: 19 May 2025 | **Revised:** 29 July 2025 | **Accepted:** 31 July 2025

Funding: This study was funded by the Ministerio de Ciencia, Innovación y Universidades/Agencia Estatal de Investigación/10.13039/501100011033, the European Social Fund Plus (PRE2022-102574, Project CEX2021-001159-M-20-4), the Secretaría de Ciencia, Humanidades, Tecnología e Innovación (CVU867306), and the Agency for Management of University and Research Grants of the Catalan Government (2021SGR00366).

Keywords: brain maturation | fALFF | fMRI | neurodevelopment | ReHo | resting-state | VMHC

ABSTRACT

Understanding functional brain development during childhood and adolescence is essential for identifying typical neurodevelopmental trajectories. While resting-state fMRI (rs-fMRI) has become a key tool in developmental neuroscience, few studies have jointly examined multiple functional metrics to comprehensively characterize typical brain maturation across youth. We analyzed rs-fMRI data from 395 neurotypical participants aged 6–20 years from the ABIDE I and II datasets. Voxel-wise analyses were conducted using three complementary rs-fMRI metrics: fractional amplitude of low-frequency fluctuations (fALFF), regional homogeneity (ReHo), and voxel-mirrored homotopic connectivity (VMHC). Data were harmonized across sites using ComBat and CovBat methods implemented in DPABI to minimize scanner-related variability. Correlation analyses and ANOVA/ANCOVAs were performed to examine developmental age effects. Our results revealed a general pattern of declining local and interhemispheric connectivity with increasing age, across all measures. fALFF decreases were most pronounced in the medial orbitofrontal, caudate, medial occipital cortex, and cerebellum (peak $r = -0.210$); ReHo showed reductions in the insula and caudate (peak $r = -0.169$); and VMHC declines were observed in the putamen, cerebellum, superior parietal lobules, and caudate (peak r range $= -0.206$ to -0.187). These findings outline a developmental trajectory characterized by increasing functional integration and network specialization from late childhood through adolescence. The combined use of fALFF, ReHo, and VMHC provides a robust multitechnical framework for characterizing typical brain development and offers a valuable benchmark for identifying developmental deviations in clinical populations.

1 | Introduction

In recent years, we have witnessed an increasing number of publications describing early brain functional development. Childhood and adolescence represent critical periods for brain development, while also marking a period of heightened vulnerability to altered cognitive states and psychopathology (Wainberg et al. 2022). In fact, 75% of psychiatric conditions emerge during childhood and adolescence (Uddin et al. 2025). A substantial body of evidence has repeatedly demonstrated that atypical patterns of brain connectivity in children and adolescents are associated with conditions such as autism (Li et al. 2024), attention deficit hyperactivity disorder (Soman et al. 2023), dyscalculia (Mateu-Estivill et al. 2024), among

Summary

- Three complementary rs-fMRI metrics (fALFF, ReHo, VMHC) reveal a converging developmental pattern of decreased connectivity: age-related increases in local synchronization and decreases in interhemispheric connectivity.
- Results underscore the prolonged functional maturation of prefrontal regions during adolescence.
- This work offers a voxel-wise benchmark of typical functional development across metrics.

others. The number of publications on clinical populations undoubtedly exceeds the number of studies on typical development. There is substantial knowledge regarding brain development across various clinical conditions (Zhang et al. 2021); however, our understanding of developmental patterns that characterize typical neurodevelopment in children remains limited.

Understanding individual variability in brain typical development is thought to be crucial for addressing key questions in developmental neuroscience (Mills et al. 2021). This knowledge is essential for identifying individuals who diverge from typical neurodevelopmental trajectories and for tailoring prevention and intervention strategies to target the most dynamic neural processes during different stages of development. Resting-state fMRI (rs-fMRI) has become a widely used and valuable tool for investigating neural development in the human brain (Li et al. 2019; Welvaert and Rosseel 2014). This method reveals intrinsic activity of the brain neural networks through spontaneous fluctuations in the blood oxygen level-dependent (BOLD) signal (Biswal et al. 1995; Fox and Raichle 2007). Rs-fMRI assesses BOLD signal at rest and serves as a robust noninvasive method for examining brain functional connectivity in the absence of external inputs (Razi and Friston 2016). It is particularly relevant for the pediatric population because (a) it does not require participants to perform any specific task, thereby minimizing variability related to task performance, compliance, or cognitive load; this allows for the examination of intrinsic brain activity under standardized conditions across individuals; and (b) data acquisition is easy and fast, requiring less participant collaboration (Bernal 2022; Whitfield-Gabrieli et al. 2020).

A central objective of developmental neuroscience is to characterize the patterns of brain maturation. Thus, mapping brain changes during development provides valuable insights into the complex process of typical neurodevelopment and into the mechanisms that may underlie divergent cognitive and behavioral trajectories (Ouyang et al. 2024). Therefore, understanding age-related changes in brain functioning could provide insights into the mechanisms underlying typical maturation and the neurobiological underpinnings of developmental variability.

Functional coordination in the brain can be assessed using BOLD signal-based metrics such as voxel-mirrored homotopic connectivity (VMHC), which captures interhemispheric coordination. Additionally, local functional activity and synchronization can be evaluated using amplitude of low-frequency fluctuations (ALFF) and regional homogeneity (ReHo), respectively.

ALFF measures the spontaneous activity amplitude of brain regions during resting state by calculating the average square root of the power spectral density within a specific low-frequency range (Yang et al. 2007). As ALFF appears to be sensitive to physiological noise, Zou et al. (2008) proposed the fractional amplitude of low-frequency fluctuations (fALFF), a low-pass filter of ALFF that significantly reduces the sensitivity of ALFF to physiological noise and increases its sensitivity and specificity in detecting spontaneous brain activities. ReHo computes Kendall's coefficient of concordance (KCC) to measure the temporal synchronization of the nearest time series and then maps local spontaneous neural activity (Zang et al. 2004). VMHC quantifies interhemispheric functional connectivity by assessing the synchrony of spontaneous activity between mirrored voxels in both hemispheres. It reflects the degree of bilateral coordination, making VMHC central to brain information integration. This metric was originally created by Zuo et al. (2010) to measure age-related changes in development.

All three metrics have been widely validated measures of brain activity at rest, and they have been successfully applied to both typically developing (TD) children and adolescents (Figueroa-Jiménez et al. 2024; Tarchi et al. 2023; Wang, Zhao, et al. 2019), as well as to clinical pediatric populations (Li et al. 2024; Zhou et al. 2018). Nonetheless, their application to pediatric populations remains at an early stage, as most studies employing the aforementioned measures have focused on adult cohorts (Deng et al. 2022; Montalà-Flaquer et al. 2023). What is clear is that these three approaches seem to be complementary and have been recently combined to study brain intrinsic activity. In fact, Zhu et al. have reliably combined fALFF, ReHo, and VMHC in adult samples with schizophrenia (Zhu et al. 2018) and depression (Zhu et al. 2019); but still, they have not been combined to study pediatric or healthy populations.

Taken together, there is still a gap in our understanding of neurodevelopmental patterns of brain connectivity that best support typical functional maturation. As such, little work has been done at the whole-brain level to assess brain activation patterns that might reflect differing neurodevelopmental trajectories. More knowledge is needed regarding whole-brain activation at rest in TD children and adolescents and what metric of rs-fMRI provides more valuable information.

To properly investigate this, we applied fALFF, ReHo, and VMHC strategies (a) to find the resting-state activation patterns at rest that best characterize typical neurodevelopment, (b) to uncover the age effect in brain activity throughout typical development, and (c) to identify differences in spontaneous brain activity among participants of different age groups from early childhood to late adolescence in a large sample of 6–20-year-old participants from the ABIDE I and ABIDE II datasets. To the best of our knowledge, this is the first study to integrate fALFF, ReHo, and VMHC in a sample of TD children and adolescents.

2 | Methods

2.1 | Participants

We used the available Autism Brain Imaging Data Exchange (ABIDE, http://fcon_1000.projects.nitrc.org/indi/abide/) dataset for the present study. The ABIDE initiative includes two collections: ABIDE I (Di Martino et al. 2013) and ABIDE II (Di Martino et al. 2017) datasets that aggregate rs-fMRI and anatomical MRI data from multiple research sites. It was designed to facilitate the study of brain connectivity in individuals with autism spectrum disorder (ASD) and TD controls. In accordance with the ethics board policies, our study was exempt from ethical review. Details regarding acquisition parameters, informed consent procedures, diagnostic criteria, and site-specific protocols are available on the database website.

The sample consisted of TD participants from the ABIDE I and II datasets. To enhance the robustness of subsequent statistical analyses, only datasets meeting the following criteria were included: (1) participants aged 6–20 years, (2) reported IQ assessment with a standardized score, and (3) a rs-fMRI protocol in which participants were awake with eyes open, fixed on a cross, and (4) a minimum sample size of 20 participants per dataset. In this study, we included 10 collection sites (ABIDEI-KKI, ABIDEI-SDSU, AIBDEI-UCLA_1, ABIDEI-UM_1, ABIDEI-UM_2, ABIDEII-KKI_1, ABIDEII-NYU_1, ABIDEII-OHSU_1, ABIDEII-SDSU_1 ABIDEII-TCD_1). This initial sample consisted of 446 TD children and adolescents.

Following the initial selection, a quality control (QC) procedure was carried out in two steps. First, using visual inspection with the DPABI Quality Control Tool, participants were excluded if they exhibited severe head motion in the T1-weighted image, poor functional image coverage, or misregistration between structural and functional images. Due to this visual inspection control, 39 participants were excluded. Second, the mean movement value was estimated with Jenkinson's framewise displacement (FD; Jenkinson et al. 2002). Following the criteria proposed by Yan et al. (2013), subjects whose FD exceeded the group mean plus two standard deviations were excluded. As a result, 12 participants were excluded due to excessive head motion. After the entire QC, the final sample comprised 395 TD participants aged 6–20 years (110 females, 285 males; $M = 11.89 \pm 2.94$ years).

For subsequent analyses aimed at detecting age-specific differences using ANOVA/ANCOVA, a subsample of 384 healthy participants aged 7–19 years was selected. This sample was divided into six discrete age groups in steps of 2 years: 7–8.99 years ($n = 39$), 9–10.99 years ($n = 130$), 11–12.99 years ($n = 102$), 13–14.99 years ($n = 51$), 15–16.99 years ($n = 32$), and 17–19 years ($n = 30$). The age intervals were chosen to capture subtle developmental transitions across relatively narrow age spans, which is particularly relevant in the context of adolescence, where brain maturation occurs rapidly and nonlinearly. This categorization is consistent with prior neurodevelopmental research and aligns with the recommendations of Sala-Llonch et al. (2015) and Xu et al. (2021), who advocate for fine-grained age groupings to enhance sensitivity to developmental changes in functional brain architecture, maximize age resolution while ensuring statistical power by keeping at least 10 subjects for each group.

2.2 | fMRI Data Preprocessing

Image preprocessing was conducted using the Data Processing Assistant for rs-fMRI (DPARSF; Yan and Zang 2010). This pipeline, implemented in MATLAB, is based on SPM12 (http://www.fil.ion.ucl.ac.uk/spm) and DPABI (http://rfmri.org/DPARSF). Initially, the first 10 functional volumes were discarded to minimize potential effects related to participants adapting to the scanner and to allow for proper magnetization equilibrium. The remaining functional images underwent slice-timing correction based on their acquisition times, followed by head motion estimation. Nuisance signals, including white matter (WM) and cerebrospinal fluid (CSF) fluctuations, linear trends, and the 24 Friston head-motion parameters (Friston et al. 1996), were regressed out. Subsequently, functional images were co-registered to their respective structural images, which were then segmented and normalized to Montreal Neurological Institute (MNI) 152 space using Diffeomorphic Anatomical Registration Through Exponentiated Lie (DARTEL) (Ashburner 2007). Functional images were also normalized to MNI space via the computed warping parameters and resampled to 3 mm isotropic voxels. To improve intersubject alignment, anatomical images were normalized to MNI space using the DARTEL algorithm implemented in DPABI. This method has been widely used in large-scale developmental neuroimaging studies and has demonstrated high registration accuracy across diverse age ranges, including children and adolescents (Guo et al. 2019; Ingalhalikar et al. 2021; Kim et al. 2021; Ma et al. 2026; Ruan et al. 2024). For ReHo analysis, the normalized functional images were subjected to bandpass filtering (0.01–0.1 Hz).

2.3 | Voxel-Based Morphometry

The T1w-structural images were automatically processed with DPABI (Yan et al. 2016). The images were reoriented and individually checked for QC. Afterward, reoriented T1 images were segmented into gray matter (GM), WM, and CSF (Ashburner and Friston 2005). Finally, the DPABI module uses the DARTEL algebra tool (Ashburner 2007) to compute transformations from individual native space to MNI space. GM segmentations were resliced and smoothed to match the parameters with the functional images. Additionally, total gray matter volumes (GMV) and parcellation volumes were calculated using SPM12 and SPM12-based scripts (Maldjian et al. 2003, 2004).

2.4 | Harmonization

We use DPABI Harmonization (Wang et al. 2024) to reduce the potential biases and nonbiological variability induced by site and scanner effects. The selected method was ComBat (Fortin et al. 2017, 2018; Johnson et al. 2007)/CovBat (Chen, Beer, et al. 2021).

ComBat harmonization was performed using a parametric approach without covariate adjustment, ensuring that site-related variability was removed while retaining a meaningful biological signal. CovBat was further applied to address site-related effects in covariance structures, improving the harmonization of functional connectivity measures. For CovBat, we employed the parametric method and set the principal component analysis (PCA) covariance threshold to 90%, following recommendations for optimizing site effect removal while maintaining biological signal integrity.

2.5 | Estimation of fALFF, ReHo, and VMHC Values

The estimation of fALFF, ReHo, and VMHC values was conducted using DPABI. For fALFF computation, the voxelwise data were spatially smoothed with a 4 mm full-width at half-maximum (FWHM) Gaussian kernel. The time series of each voxel was then transformed into the frequency domain using a fast Fourier transform (FFT) to derive the power spectrum. ALFF values were obtained by computing the square root of the power spectrum within the 0–0.25 Hz range and averaging the values across the 0.01–0.08 Hz frequency band for each voxel. Subsequently, fALFF was derived by normalizing ALFF values to the total power across the full frequency range (0–0.25 Hz; Zou et al. 2008).

ReHo was estimated by calculating KCC for the time series of each voxel and its 27 neighboring voxels (Zang et al. 2004). The resulting ReHo maps were then smoothed using a 4 mm FWHM Gaussian kernel. Both fALFF and ReHo maps were standardized into z-score maps by subtracting the mean and dividing by the standard deviation.

For VMHC computation, after normalization, the processed images underwent spatial smoothing using an 8 mm FWHM Gaussian kernel, followed by linear detrending and bandpass filtering (0.01–0.1 Hz). A symmetric normalized MNI152 template provided by the DPABI toolbox was employed to ensure bilateral anatomical alignment. VMHC was calculated using the Pearson correlation coefficient (Fisher z-transformed) between the time series of each voxel and its mirrored interhemispheric counterpart was computed, yielding a subject-specific VMHC map. Further details on VMHC computation can be found in prior research (Zuo et al. 2010).

2.6 | Statistical Analyses

All statistical analyses for fALFF, ReHo, and VMHC were conducted using DPABI.

Correction for multiple comparisons was performed using Gaussian Random Field (GRF) theory, following the recommendations by Eklund et al. (2016), with a voxel-level threshold of $p < 0.01$ and a cluster-level threshold of $p < 0.05$. Additionally, to exclude very small clusters that may survive correction but lack anatomical reliability, we applied metric-specific minimum cluster size thresholds following voxel-wise statistical correction. For fALFF, we applied a minimum extent threshold of 10 voxels, consistent with previous task-based and resting-state studies using similar parameters for BOLD signal amplitude measures (He et al. 2024; Montalà-Flaquer et al. 2024; Tommasin et al. 2017). For ReHo, a minimum cluster size of 30 voxels was applied in line with recommendations from both foundational studies on ReHo (Zang et al. 2004) and more recent clinical applications (Huck et al. 2023; Montalà-Flaquer et al. 2024; Wang et al. 2025). Finally, for VMHC, we applied a threshold of 20 voxels, based on methodological precedents in developmental and clinical neuroimaging research that highlight the need for intermediate cluster sizes to capture robust interhemispheric synchrony (Chen, Sun, et al. 2021; Xu and Zhang 2023). These cluster size criteria were selected to balance sensitivity and anatomical specificity across metrics with differing signal properties and spatial characteristics.

To assess the linear relationship between brain measures and chronological age, voxel-wise Pearson correlation analyses were performed separately for each metric (fALFF, ReHo, and VMHC) across the whole brain. Pearson correlation coefficients were computed only after confirming the linearity of the relationships between age and rs-fMRI measures. Linearity was assessed through Q–Q plots, validating the use of Pearson's method.

These analyses were conducted across the full sample ($n = 395$). To account for structural variation across participants during development, GMV was included as a covariate in all models. This decision was informed by prior research, particularly in the context of healthy aging (Feis et al. 2019; Hafkemeijer et al. 2013; Hoffstaedter et al. 2015; Montalà-Flaquer et al. 2023), and also in developmental samples (Figueroa-Jiménez et al. 2024; Jolles et al. 2011; Porcu et al. 2019; Tapia-Medina et al. 2025). In addition, to test the robustness of our findings, we also conducted parallel models without GMV as a covariate. Correction for multiple comparisons followed GRF theory as described above.

To further explore age-related differences in brain function and identify specific developmental stages, voxel-wise one-way ANCOVA (with GMV as covariate) and ANOVAs (without covariate) were conducted using a subsample of participants with available data across six discrete age groups ($n = 384$): Group 1 (G1, 7–9 years), G2 (9–11 years), G3 (11–13 years), G4 (13–15 years), G5 (15–17 years), and G6 (17–19 years). Post hoc comparisons between age groups were performed using Tukey's HSD test to identify pairwise differences within significant clusters. This grouping strategy was conceptually motivated by evidence of nonlinear, stage-specific changes in brain maturation during childhood and adolescence (Sala-Llonch et al. 2015; Xu et al. 2021). Recent meta-analytic findings further support the use of neurodevelopmentally informed age bins over equal-sized divisions, as they may enhance the sensitivity and interpretability of group-level comparisons in functional imaging (Tapia-Medina et al. 2025).

Significant clusters were localized in standard MNI space, and their corresponding anatomical labels were identified using the Automated Anatomical Labeling (AAL) atlas (Tzourio-Mazoyer et al. 2002). Visualization of statistical maps was performed using DPARSF (Yan and Zang 2010).

TABLE 1 | Significant correlations between fALFF, ReHo, and VMHC maps, with age, respectively.

			VBM covariate		No VBM covariate	
Brain region	**BA**	**MNI coordinates**	**Peak *r* value**	**Cluster size**	**Peak *r* value**	**Cluster size**
fALFF						
Frontal Med Orb L	10	−6, 69, −6	−0.210	181	−0.209	163
ReHo						
~Insula R	13	33, −21, 6	−0.169	115	—	—
VMHC						
Putamen R	49	24, 12, 12	−0.187	322	−0.186	311
Putamen L	49	−24, 12, 12	−0.188	305	−0.186	311
~Frontal Mid R	6	36, 6, 66	−0.206	205	−0.205	197

Note: All results survived GRF correction for multiple comparisons (voxel-level $p < 0.01$, cluster-level $p < 0.05$).
Abbreviations: ~, Approximately; AAL, atlas area closer to the *t* peak; L, left; *R*, right; BA, Brodman area; MNI, Montreal Neurological Institute.

3 | Results

Voxel-wise analyses of rs-fMRI metrics revealed multiple significant effects of age on brain function in neurotypical participants aged 6–20 years ($n = 395$ for correlation analyses; $n = 384$ for group comparisons). All results survived GRF correction for multiple comparisons (voxel-level $p < 0.01$, cluster-level $p < 0.05$), and are described below for each metric.

3.1 | fALFF Results

In the voxel-wise correlation analyses, a significant negative association between age and fALFF is observed in the left medial orbitofrontal cortex (mOFC) ($r = -0.210$ with GMV). Table 1 lists the brain regions showing significant associations between fALFF and age for both approaches, with and without GMV covariate. Figure 1 provides a visual representation of the main clusters. The corresponding scatterplots illustrating the relationship with age are presented in Figure 2.

Regarding ANOVA/ANCOVA analyses, participants aged 7–9 years (G1) exhibit higher fALFF compared to older groups, particularly within the fusiform gyrus, the bilateral caudate, the mOFC, the anterior cingulate cortex, and occipital middle gyrus. Furthermore, certain age group comparisons such as G2 versus G6 and G3 versus G6 highlight significant decreases with age within cerebellar regions and thalamic nuclei. The details of each between-group comparison are portrayed in Table 2 and Figure 3. To ensure visual clarity, Figure 3 only includes the brain images from G6 comparisons, as they are the most representative of the overall pattern. The remaining images from the comparisons can be found in Figures S1–S4.

3.2 | ReHo Results

A significant negative correlation between ReHo and age was found in the right insula, showing a decrease in local functional synchrony across development ($r = -0.169$ with GMV covariate). Table 1 shows a detailed localization of this cluster. Figures 1 and 2 graphically show the representation of these results.

ANOVA/ANCOVA reveals that 7–9 years participants (G1) exhibit increased ReHo values compared to the oldest group (G6) in the left caudate. Similarly, we observe increased ReHo values in the G4 compared to the G5 within the pallidum and right thalamus. Conversely, we observe reduced ReHo values in the G4 compared to the G5 within the pallidum and right thalamus. These results are presented in Table 3, as well as in Figure 4.

3.3 | VMHC Results

Age was negatively correlated with VMHC in the right middle frontal gyri ($r = -0.206$ with GMV covariate) and the putamen ($r = -0.187$ with GMV covariate). Table 1 shows a detailed localization of the three clusters. Figures 1 and 2 graphically show the representation of these results.

The ANOVA/ANCOVA analyses for VMHC indicate a decreasing pattern of interhemispheric connectivity with age. In the comparison between G1 (7–9 years) and G6 (17–19 years), younger participants exhibited significantly greater VMHC in the cerebellum and the caudate. Likewise, comparisons between intermediate groups (e.g., G2 vs. G5, G2 vs. G6, G3 vs. G6) also revealed significant decreases in VMHC with age, particularly in the cerebellum, the caudate, superior parietal lobules, and the putamen. The details of each between-group comparison are presented in Table 4 and Figure 5. As with fALFF, Figure 5 only displays brain images from G6 comparisons. The remaining images from the comparisons can be found in Figure S5.

4 | Discussion

In the present study, based on rs-fMRI data from a multisite sample of TD children and adolescents, we explored (1) the association between age and fALFF, ReHo, and VMHC, and (2) between-group differences among six groups of age—from childhood to late adolescence—using the mentioned measures of brain spontaneous activity. Although the three rs-fMRI metrics yielded partially distinct spatial patterns, this divergence is expected given their different analytical purposes and

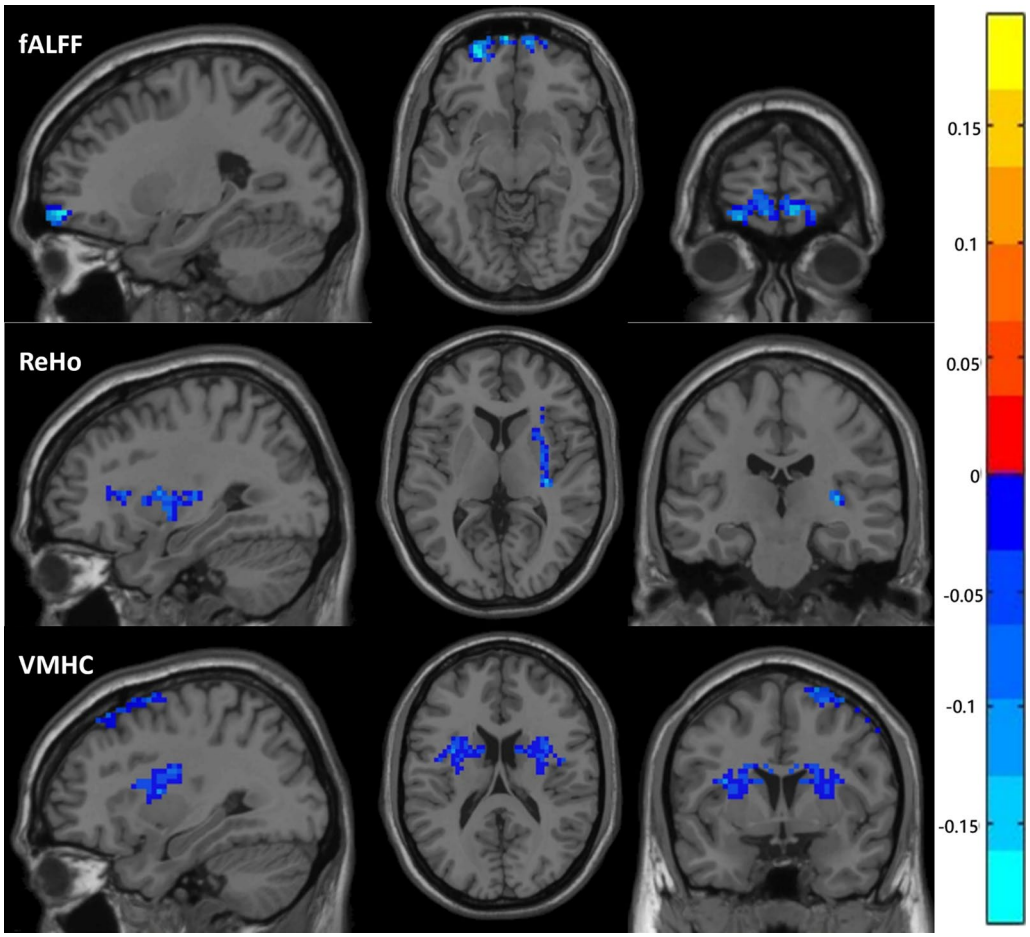

FIGURE 1 | Sagittal, axial, and coronal planes representation of significant correlations between fALFF, ReHo, and VMHC whole-brain maps with age. The color bar indicates the value of the correlation (*r*), with yellow representing positive correlations and blue representing negative correlations. These images were constructed with the GMV covariate, given their close similarity with those from the unadjusted models.

neurophysiological sensitivities: fALFF reflects the amplitude of spontaneous low-frequency activity, ReHo captures local synchrony, and VMHC quantifies interhemispheric coordination. Nevertheless, all three consistently revealed a general developmental trend of decreased intrinsic connectivity with age. This convergence, despite methodological differences, supports the robustness of the findings.

The present findings align with and extend previous research aiming to characterize typical patterns of brain development using rs-fMRI. Consistent with the notion that childhood and adolescence are periods of intense neurodevelopmental change (Mills et al. 2021; Wainberg et al. 2022), our results revealed a general pattern of declining local and interhemispheric connectivity with increasing age, across all measures. The observed reduction in intrinsic connectivity with age aligns with previous developmental research. Içer (2019) identifies less connectivity links with age, and FC between-networks decreases in healthy 8–18-year-old participants. Similarly, Marek et al. (2015) describe a decrease in global connectivity strength both within and between networks from childhood to late adolescence. Specifically, in our work, significant connectivity decreases were predominantly observed in regions involved in higher-order cognitive and sensory processing. Notably, reductions in fALFF were observed in the fusiform gyrus, mOFC, anterior cingulate cortex, caudate nuclei, and middle occipital cortex. The mOFC, a key node of the Default Mode Network (DMN), is involved in affective processing, decision-making, and self-referential thought (Wang, Yue, et al. 2019). This finding is consistent with previous studies indicating that the DMN undergoes significant reorganization during adolescence, reflecting the maturation of self-referential and social cognitive processes (Betzel et al. 2014; Supekar et al. 2010). In line with our findings, Loh and Ronsenkranz (2022) found that the number of mOFC neurons decreases during development. The fusiform gyrus, also enhanced in younger participants, supports social perception and face processing, functions that undergo refinement throughout development (Grill-Spector et al. 2018). Tian et al. (2023) observed that, compared to adolescents, children exhibited increased connectivity degree centrality in the left dorsolateral fusiform gyrus. This maturation likely reflects the refinement of neural circuits involved in social cognition.

Subcortical regions, including the caudate, thalamus, cerebellum, and putamen, also demonstrated decreased activity with age, in all three metrics. The caudate nucleus, part of the basal ganglia network, plays a crucial role in procedural learning, cognitive control, and goal-directed behavior. Its developmental trajectory suggests a shift from diffuse to more focused activation

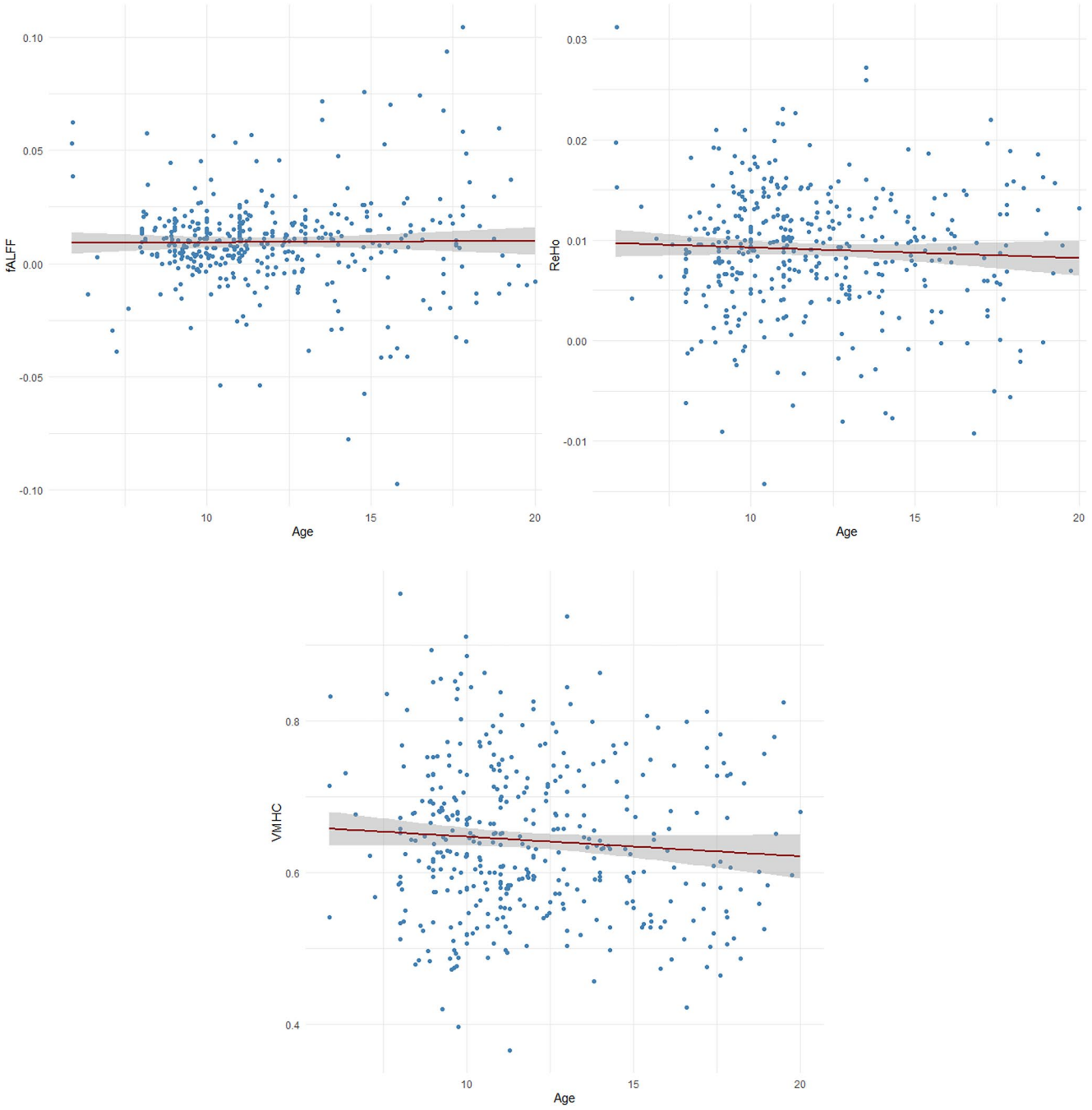

FIGURE 2 | Scatterplots of significant correlations between fALFF, ReHo, and VMHC whole-brain maps with age. From left to right, the scatterplots depict the correlations between age and fALFF, ReHo, and VMHC, respectively. These images were generated controlling for GMV.

patterns, indicative of increasing efficiency in cognitive processing. Similarly, the thalamus serves as a relay center for sensory and motor signals and is integral to attentional modulation (Ferguson and Gao 2015). Age-related changes in thalamic connectivity may reflect the maturation of attentional networks and sensory integration processes. This pattern of decreased subcortical connectivity with advancing age in childhood and adolescence is well documented in the literature (Langen et al. 2018; Sato et al. 2015). In a similar age-range sample to ours, Sanders et al. (2023) describe FC decreases in the cerebellar-striatal-thalamic circuits.

Age-related decreases in VMHC were particularly prominent in regions such as the bilateral putamen, cerebellum, and superior parietal lobules. These areas are functionally diverse but share a role in motor coordination, working memory, and cognitive control. The putamen, a subcortical structure within the basal ganglia, is involved in motor planning and habit learning, while the cerebellum supports not only motor functions but also timing, prediction, and emotional regulation (Boonstra 2025). The superior parietal lobule, part of the dorsal attention network, facilitates visuospatial attention and sensorimotor integration. VMHC decrease is consistent with the findings by Tarchi

TABLE 2 | Significant age group comparisons in fALFF.

			VBM covariate		No VBM covariate	
Brain region	**BA**	**MNI coordinates**	**Peak *t* value**	**Cluster size**	**Peak *t* value**	**Cluster size**
G1 vs. G2						
Fusiform_L	38	−24, 0, −39	4.482	18	4.489	18
Frontal Mid Orb R	10	39, 51, −12	3.350	12	3.354	12
Caudate L	48	−9, 15, 3	3.404	14	3.410	14
~Caudate R	24	6, 21, 12	3.227	21	—	—
Caudate R	48	9, 18, 12		—	3.232	21
Occipital Mid L	19	−33, −90, 24	3.634	17	3.636	17
G1 vs. G3						
Fusiform L	36	−24, −3, −39	3.634	10	3.639	10
Occipital Mid L	19	−33, −90, 24	3.118	15	3.120	15
G1 vs. G4						
~Fusiform L	36	−21, −3, −39	3.388	12	3.383	12
Frontal Mid Orb R	10	36, 54, −15	2.768	17	2.753	18
Frontal Mid Orb L	10	−27, 66, −9	3.190	10	—	—
Frontal Sup Medial L	10	−12, 54, 9	3.642	12	3.649	12
G1 vs. G5						
Temporal Mid L	38	−51, 0, −21	3.326	16	3.332	16
Temporal Mid R	21	57, −15, −18	2.972	11	2.960	11
Frontal Med Orb L	10	−6, 69, −6	4.101	13	4.109	13
Occipital Mid L	19	−33, −90, 24	3.454	21	3.456	21
Frontal Sup Medial L	9	−3, 45, 45	−3.066	15	—	—
Frontal Sup Medial L	8	−3, 42, 48	—	—	−3.069	15
G1 vs. G6						
Frontal Med Orb R	10	9, 66, −6	2.912	10	2.912	10
Caudate L	48	−6, 18, 3	3.730	40	3.712	39
Cingulum Ant L	32	−9, 45, 6	3.071	17	3.022	17
G2 vs. G3						
~Thalamus L	50	−6, −27, 12	−3.886	11	−3.888	11
G2 vs. G6						
~Cerebelum 7b R	19	15, −78, −54	3.748	73	3.747	73
~Cerebelum 7b L	19	−30, −72, −54	3.107	54	—	—
~Cerebelum 7b L	19	−33, −72, −54	—	—	3.109	54
Frontal Inf Orb R	47	39, 27, −6	−3.243	16	−3.244	16
G3 vs. G4						
Fusiform R	37	33, −69, −15	−3.419	17	−3.424	17
G3 vs. G5						
Frontal Sup Orb R	11	15, 21, −18	3.088	15	3.093	15

(Continues)

TABLE 2 | (Continued)

Brain region	BA	MNI coordinates	VBM covariate		No VBM covariate	
			Peak *t* value	Cluster size	Peak *t* value	Cluster size
G3 vs. G6						
Cerebelum 8 R	19	15, −75, −54	3.187	17	3.191	17
~Cerebelum 7b L	19	−27, −72, −54	3.332	31	3.333	31
~Thalamus L	50	−3, −24, 12	3.770	28	3.774	28
Frontal Mid L	6	−36, 3, 51	−2.854	12	—	—
G4 vs. G5						
Cerebelum 8 R	19	12, −72, −51	−3.040	25	−3.046	25
~Precentral R	6	39, 0, 33	3.276	16	3.149	16
Precentral L	6	−30, −3, 63	−3.680	18	−3.685	18
G4 vs. G6						
Cerebelum 6 R	37	39, −63, −21	2.895	13	2.900	13
Supp Motor Area R	6	12, −6, 75	3.403	18	3.408	19
G5 vs. G6						
Cerebelum 7b R	19	15, −78, −51	4.441	222	4.366	221

Note: G1 (7–9 years), G2 (9–11 years), G3 (11–13 years), G4 (13–15 years), G5 (15–17 years), and G6 (17–19 years). All results survived GRF correction for multiple comparisons (voxel-level $p < 0.01$, cluster-level $p < 0.05$); AAL atlas area closer to the *t* peak.
Abbreviations: ~, approximately; BA, Brodmann area; L, left; MNI, Montreal Neurological Institute; *R*, right.

et al. (2023), who report a gradual decline in interhemispheric interactions with age. The developmental decline in interhemispheric connectivity within these regions suggests a transition toward hemispheric specialization and more lateralized processing strategies, consistent with typical patterns of adolescent brain maturation (Tarchi et al. 2023; Zuo et al. 2010).

The observed reductions in fALFF and VMHC values with age—particularly within subcortical, occipital, and frontal midline regions—support the hypothesis of a progressive decrease in baseline neural synchrony and bilateral coupling, reflecting increased network specialization and functional differentiation throughout adolescence. These findings are in line with previous reports of declining interhemispheric connectivity (Zuo et al. 2010) and localized reductions in intrinsic activity (Figueroa-Jiménez et al. 2024; Wang, Zhao, et al. 2019) but uniquely contribute to the field by demonstrating these patterns simultaneously across fALFF, ReHo, and VMHC within the same sample.

Moreover, the use of a multitechnical analytical approach enabled the identification of subtle but meaningful exceptions to these trends, such as the relative preservation of VMHC in associative parietal regions or ongoing decreases in fALFF within cerebellar structures, highlighting region-specific and potentially nonlinear developmental trajectories. These nuances are critical, as they suggest that typical neurodevelopment is not characterized by a uniform progression, but rather by dynamic and heterogeneous shifts in network architecture that vary by brain region and function.

Notably, consistent age-related decreases were observed in cerebellar regions across all three rs-fMRI metrics, particularly within posterior lobules such as Crus 2 and lobule 7b. These findings are in line with a growing body of literature positioning the cerebellum as a central hub not only for motor coordination but also for cognitive and affective development (Boonstra 2025; Buckner et al. 2011; Stoodley and Schmahmann 2009). Specifically, posterior cerebellar regions are structurally and functionally connected with prefrontal and parietal association cortices, supporting higher-order functions including working memory, social cognition, timing, internal modeling, and emotional regulation (Mastrangelo et al. 2024). Our results suggest that cerebellar contributions to brain maturation extend beyond childhood into adolescence and that developmental changes in cerebello-cortical functional coupling may reflect increasing specialization of these integrative processes. These findings also highlight the value of including the cerebellum in developmental neuroimaging pipelines, as its systematic exclusion in some studies may hinder a comprehensive understanding of whole-brain maturation. By demonstrating coherent developmental patterns in cerebellar rs-fMRI activity and connectivity, our study adds to the growing recognition of the cerebellum as a key node in large-scale neurodevelopmental trajectories.

The possible explanations for the patterns we obtained in our results point toward key neurobiological mechanisms that underlie typical brain maturation. One potential explanation involves synaptic pruning, a process through which the brain selectively eliminates excess or inefficient synapses during development, promoting greater neuronal regulation and circuit refinement (Tarchi et al. 2023). This mechanism may explain reductions in fALFF or ReHo values in certain regions—not as indicators of functional loss, but rather as markers of increased specialization and efficiency. Another contributing factor could

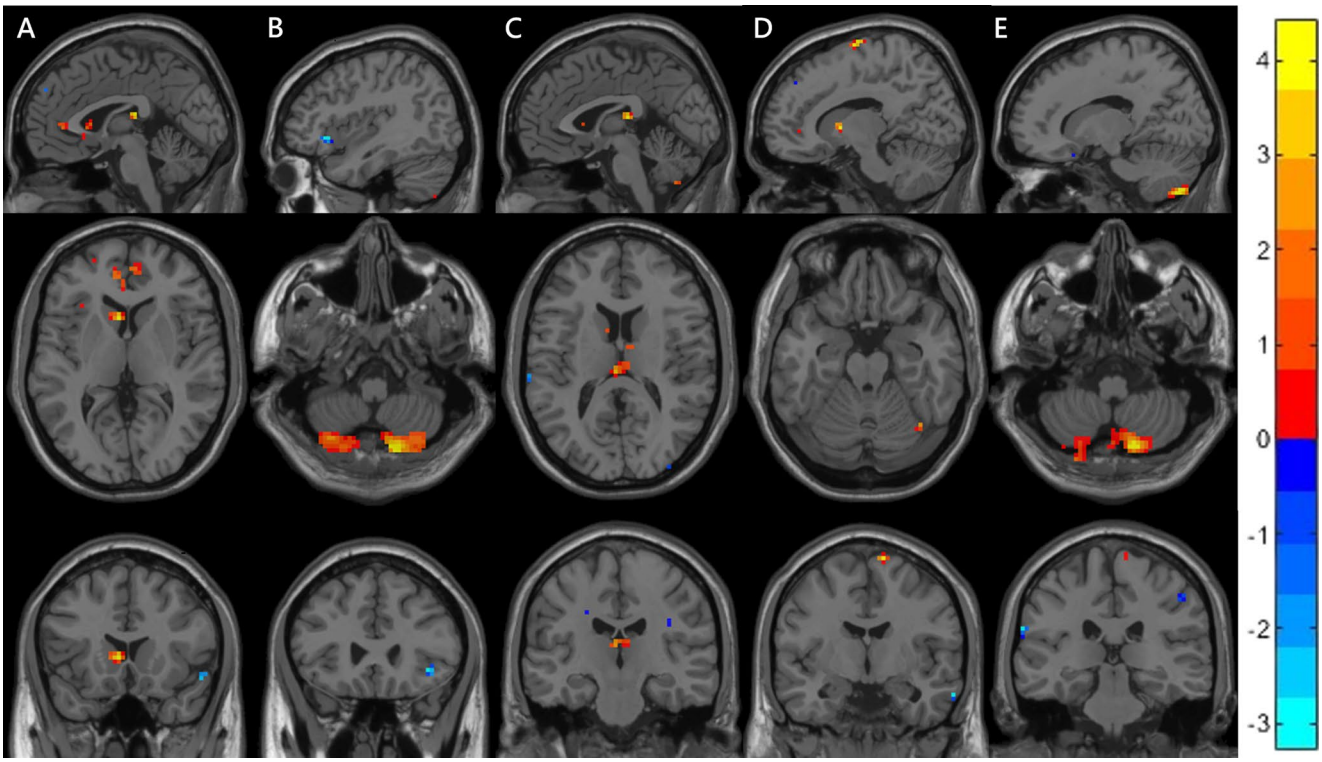

FIGURE 3 | Representation of significant fALFF differences between groups. (A) Vertically shows the sagittal, axial, and coronal planes of the significant fALFF differences between G1 and G6. (B–E) Likewise, it represents the significant differences between G2 and G5 against G6. The color bar indicates the intensity of the difference (*t*), with yellow representing positive differences and light blue representing negative differences. These images were constructed with the GMV covariate, given their close similarity with those from the unadjusted models.

TABLE 3 | Significant age group comparisons in ReHo.

			VBM covariate		No VBM covariate	
Brain region	**BA**	**MNI coordinates**	**Peak *t* value**	**Cluster size**	**Peak *t* value**	**Cluster size**
G1 vs. G6						
Caudate_L	48	–15, 3, 15	3.950	31	3.950	32
G4 vs. G5						
Thalamus_R	50	6, –18, 6	3.785	30	3.791	30
~Pallidum_L	51	–15, 0, 6	4.219	31	4.212	31
Pallidum_R	51	15, 3, 3	4.216	51	4.221	51

Note: G1 (7–9 years), G2 (9–11 years), G3 (11–13 years), G4 (13–15 years), G5 (15–17 years), and G6 (17–19 years). All results survived GRF correction for multiple comparisons (voxel-level $p < 0.01$, cluster-level $p < 0.05$); AAL atlas area closer to the *t* peak.
Abbreviations: ~, approximately; BA, Brodmann area; L, left; MNI, Montreal Neurological Institute; *R*, right.

be the increasing efficiency of large-scale neural networks with age. As the brain matures, it tends to transition from more redundant and locally driven activity toward streamlined and efficient long-range connectivity (Sanders et al. 2023). This reorganization likely underlies observed decreases in VMHC or localized activity, particularly in regions no longer requiring high levels of baseline synchrony as internetwork communication becomes more optimized. These mechanisms together highlight that brain development involves not just growth, but also selective refinement and increased efficiency across different neural systems.

Collectively, our results suggest that brain maturation from childhood through late adolescence is associated with a global reduction in local spontaneous activity (fALFF), local synchrony (ReHo), and interhemispheric connectivity (VMHC). This shift likely reflects a refinement of functional architecture that supports the emergence of specialized, efficient brain systems during adolescence. Both cortical and subcortical regions contribute to this process, particularly those implicated in executive function, emotional regulation, sensory integration, and social cognition. The findings thus provide evidence for a coordinated reorganization of functional networks underpinning

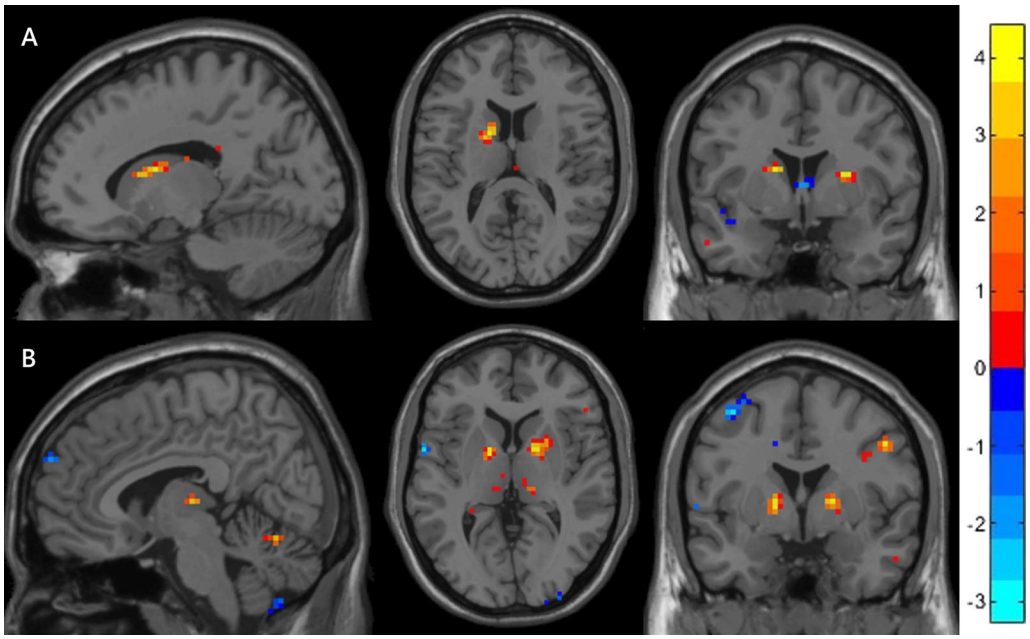

FIGURE 4 | Representation of significant ReHo differences between groups. (A) Horizontally shows the sagittal, axial, and coronal planes of the significant ReHo differences between G1 and G6. (B) Likewise, between G4 and G5. The color bar indicates the intensity of the difference (*t*), with yellow representing positive differences and light blue representing negative differences. These images were constructed with the GMV covariate, given their close similarity with those from the unadjusted models.

the cognitive and affective maturation that occurs between childhood and early adulthood.

This work has some limitations. First, this study was conducted using publicly available datasets, which did not share the same scanning protocol nor the same fMRI scanner. This represented a challenge that we attempted to address by applying harmonization techniques. Notably, the use of data harmonization procedures ensured that site-related variability was minimized, enhancing the reliability and interpretability of age-related effects across a large, multisite dataset. Second, our work has a cross-sectional design that limits our observation of changes throughout the process of brain maturation. Longitudinal approaches are more suitable when analyzing aspects of ontogenetic development. Third, we acknowledge that effect sizes are modest. However, the consistent spatial pattern across metrics and statistical analysis, as well as the alignment with established developmental frameworks, underscore the robustness of our findings. Also, it is noteworthy that we are working with a healthy population, where the effects or differences are expected to be lower than studies that compare clinical populations and controls. Finally, the number of male participants far exceeds that of female participants, which may introduce a potential bias that we did not control for, as sex differences were not a focus of this study. Interestingly, similar age-related patterns were reported by Tarchi et al. (2023), despite the fact that their sample was skewed toward females. This convergence across studies suggests that the developmental trajectories observed here are likely robust and not solely driven by sex composition.

Although this study was conducted using publicly available datasets, this work addresses a major gap in the developmental neuroscience literature, where knowledge of typical brain maturation remains limited relative to clinical populations (Uddin et al. 2025; Zhang et al. 2021). By leveraging large-scale, harmonized multisite data and a whole-brain, voxel-wise approach, we provide new evidence by establishing reference developmental patterns and supporting the value of fALFF, ReHo, and VMHC as complementary markers of typical brain development. Importantly, the study was designed with a strong emphasis on methodological rigor—employing harmonization techniques, GM volume control, strict motion control, and voxel-wise statistical corrections—which directly addresses growing concerns regarding replicability in neuroimaging research. In light of the ongoing reproducibility crisis within the field, our approach aims not only to uncover robust developmental signals but also to promote transparency and generalizability. As such, this work serves as a replicable and well-documented foundation for future investigations into both typical and atypical brain development.

5 | Conclusion

The present study provides robust evidence of age-related decreases in spontaneous brain activity and connectivity across childhood and adolescence. We observed consistent negative associations with age in regional amplitude (fALFF), local synchrony (ReHo), and interhemispheric connectivity (VMHC), particularly in association cortices. These converging findings suggest a progressive reduction in intrinsic functional activity as part of typical brain maturation from childhood to early adulthood.

Our findings contribute to a growing understanding of typical brain maturation and may serve as a reference point for identifying deviations in clinical populations. Importantly, the convergence of findings across different functional metrics strengthens

TABLE 4 | Significant age group comparisons in VMHC.

			VBM covariate		No VBM covariate	
Brain region	**BA**	**MNI coordinates**	**Peak *t* value**	**Cluster size**	**Peak *t* value**	**Cluster size**
G1 vs. G6						
~Cerebelum Crus2 L	18	−3, −87, −30	4.038	45	4.044	45
Cerebelum Crus2 R	18	3, −87, −30	4.038	39	4.044	39
~Caudate R	48	21, −6, 27	3.235	39	3.241	39
~Caudate L	48	−21, −6, 27	3.238	39	3.241	39
G2 vs. G5						
Parietal Inf R	39	60, −54, 42	3.085	21	3.086	21
G2 vs. G6						
~Cerebelum Crus2 L	18	−6, −93, −33	4.689	42	4.690	42
~Cerebelum Crus2 R	18	6, −93, −33	4.698	36	4.690	36
~Caudate R	48	21, −6, 27	3.150	30	3.155	29
~Caudate L	48	−21, −6, 27	3.153	29	3.155	29
Parietal Sup R	7	21, −63, 69	3.359	39	3.363	39
Parietal Sup L	7	−21, −63, 69	3.359	31	3.363	31
G3 vs. G6						
~Cuneus L	19	−9, −93, −36	4.271	25	4.262	25
~Frontal Inf Oper R	44	30, 3, 27	2.954	30	2.958	29
~Frontal Inf Oper L	44	−30, 3, 27	2.960	29	2.958	29
Parietal Sup L	7	−30, −60, 63	3.392	30	3.390	30
Parietal Sup R	7	30, −60, 63	3.391	38	3.390	38
G4 vs. G5						
~Cingulum Mid L	6	−21, −9, 42	4.427	39	4.433	39
~Cingulum Mid R	6	21, −9, 42	4.422	39	4.433	39
~Temporal Mid L	39	−39, −54, 21	3.911	27	3.891	27
Temporal Mid R	39	39, −54, 21	3.913	27	3.891	27
Pallidum L	51	−18, 0, 6	3.503	37	3.505	37
Pallidum R	51	18, 0, 6	3.513	37	3.505	37
G4 vs. G6						
~Cerebelum Crus2 L	18	−6, −93, −33	4.171	26	4.171	26
~Cerebelum Crus2 R	37	48, −78, −39	3.265	21	3.266	21
~Putamen R	48	21, −3, 15	3.020	22	3.019	21
~Putamen L	49	−21, −3, 15	3.024	21	3.019	21
G5 vs. G6						
Angular R	39	54, −48, 33	−3.485	25	−3.491	26
SupraMarginal L	39	−54, −48, 33	−3.523	25	−3.491	26

Note: G1 (7–9 years), G2 (9–11 years), G3 (11–13 years), G4 (13–15 years), G5 (15–17 years), and G6 (17–19 years). All results survived GRF correction for multiple comparisons (voxel-level $p < 0.01$, cluster-level $p < 0.05$); AAL atlas area closer to the *t* peak.
Abbreviations: ~, approximately; BA, Brodmann area; L, left; MNI, Montreal Neurological Institute; *R*, right.

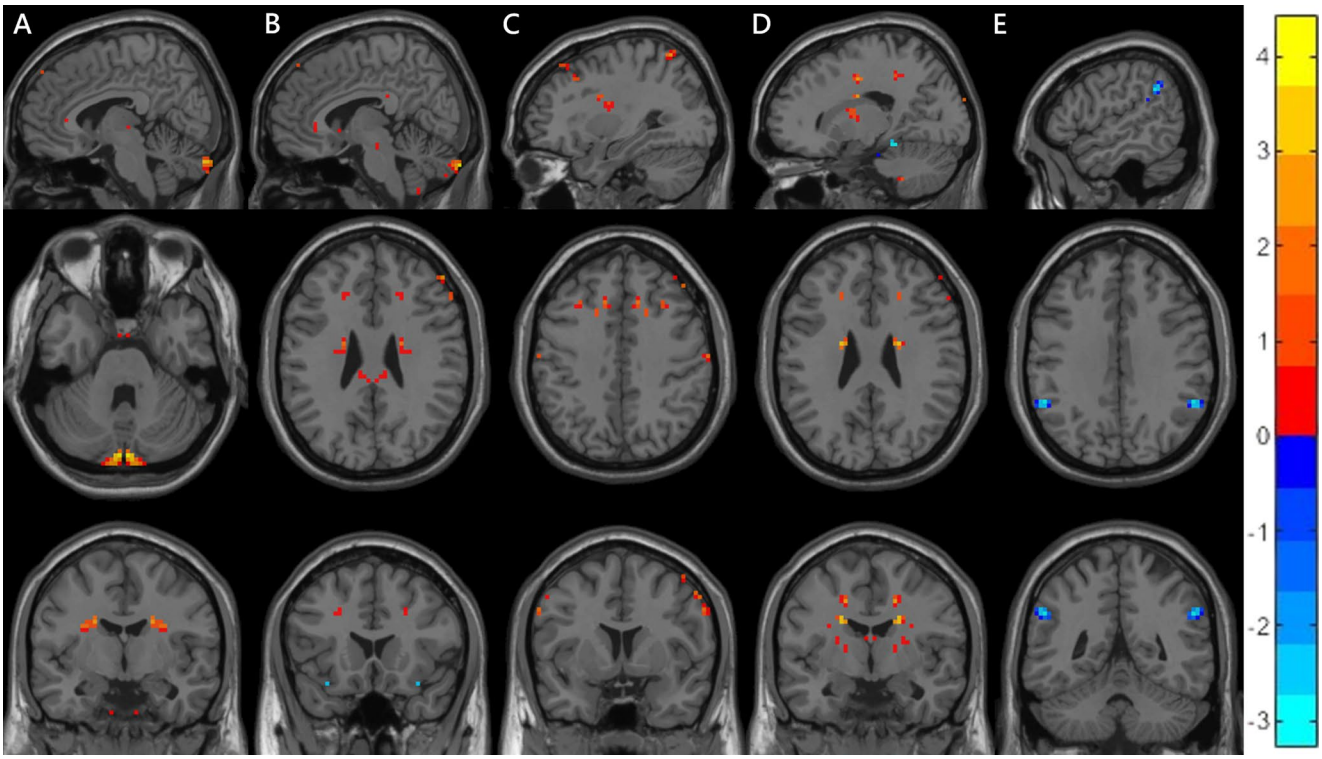

FIGURE 5 | Representation of significant VMHC differences between groups. (A) Vertically shows the sagittal, axial, and coronal planes of the significant VMHC differences between G1 and G6. (B–E) Likewise, it represents the significant differences between G2 and G5 against G6. The color bar indicates the intensity of the difference (*t*), with yellow representing positive differences and light blue representing negative differences. These images were constructed with the GMV covariate, given their close similarity with those from the unadjusted models.

the interpretation of these results, suggesting that distinct aspects of intrinsic brain function undergo parallel developmental changes. At the same time, the modest effect sizes and partial overlap between metrics highlight the complexity of brain development and the role of individual variability.

The strength of this work lies in the use of a large, harmonized, multisite sample and the integration of complementary rs-fMRI metrics, which together offer complementary perspectives on functional brain maturation. This is a solid contribution to the field, offering well-supported developmental benchmarks that are critical for understanding variations across populations. The clarity of results, careful methodological control, and theoretical grounding position this manuscript as a valuable reference for future neurodevelopmental research.

Future work, particularly studies with longitudinal designs or the inclusion of behavioral measures, will be critical to better contextualize these functional changes and to explore how they relate to cognitive, emotional, or clinical outcomes. In addition, future studies using simulation-based approaches or direct comparisons between fALFF, ReHo, and VMHC could further clarify the specific contributions and overlap of these complementary metrics. Beyond such comparative efforts, it would also be valuable to explore integrative analytical frameworks capable of combining these measures to model their interplay across development. We believe that such integration would require a dedicated methodological approach, and we propose this as a promising direction for future research. Ultimately, these findings lay essential groundwork for future studies aiming to identify early deviations from typical developmental trajectories and improve understanding of neurodevelopmental variability.

Acknowledgments

We sincerely appreciate the ABIDE project (http://fcon_1000.projects.nitrc.org/indi/abide/) for providing the publicly available data used in the current work. The authors would like to thank Ministerio de Ciencia, Innovación y Universidades/Agencia Estatal de Investigación/10.13039/501100011033 and European Social Fund Plus (Grant: PRE2022-102574, Project: CEX2021-001159-M-20-4) and the Secretaría de Ciencia, Humanidades, Tecnología e Innovación (CVU867306) for institutional support.

Ethics Statement

The studies involving humans were approved by the ABIDE I and ABIDE II projects that were carried out with approval from the local ethical committees at each participating site. The studies were conducted in accordance with the local legislation and institutional requirements.

Conflicts of Interest

The authors declare no conflicts of interest.

Data Availability Statement

The data that support the findings of this study are openly available in ABIDE I and ABIDE II at http://fcon_1000.projects.nitrc.org/indi/abide/.

References

Ashburner, J. 2007. "A Fast Diffeomorphic Image Registration Algorithm." *NeuroImage* 38, no. 1: 95–113. https://doi.org/10.1016/J.NEUROIMAGE.2007.07.007.

Ashburner, J., and K. J. Friston. 2005. "Unified Segmentation." *NeuroImage* 26, no. 3: 839–851. https://doi.org/10.1016/J.NEUROIMAGE.2005.02.018.

Bernal, B. 2022. "Practical Aspects of Functional Magnetic Resonance Imaging in Children." *Journal of Pediatric Neurology* 20, no. 2: 83–96. https://doi.org/10.1055/s-0041-1733853.

Betzel, R. F., L. Byrge, Y. He, J. Goñi, X.-N. Zuo, and O. Sporns. 2014. "Changes in Structural and Functional Connectivity Among Resting-State Networks Across the Human Lifespan." *NeuroImage* 102: 345–357. https://doi.org/10.1016/j.neuroimage.2014.07.067.

Biswal, B., F. Z. Yetkin, V. M. Haughton, and J. S. Hyde. 1995. "Functional Connectivity in the Motor Cortex of Resting Human Brain Using Echo-Planar MRI." *Magnetic Resonance in Medicine* 34, no. 4: 537–541. https://doi.org/10.1002/mrm.1910340409.

Boonstra, J. T. 2025. "The Cerebellar Connectome." *Behavioural Brain Research* 482: 115457. https://doi.org/10.1016/j.bbr.2025.115457.

Buckner, R. L., F. M. Krienen, A. Castellanos, J. C. Diaz, and B. T. T. Yeo. 2011. "The Organization of the Human Cerebellum Estimated by Intrinsic Functional Connectivity." *Journal of Neurophysiology* 106, no. 5: 2322–2345. https://doi.org/10.1152/jn.00339.2011.

Chen, A. A., J. C. Beer, N. J. Tustison, P. A. Cook, R. T. Shinohara, and H. Shou. 2021. "Mitigating Site Effects in Covariance for Machine Learning in Neuroimaging Data." *Human Brain Mapping* 43, no. 4: 1179–1195. https://doi.org/10.1002/hbm.25688.

Chen, J., D. Sun, Y. Shi, et al. 2021. "The Differences in Minimum Cluster Sizes Across Metrics Were Based on Previous Literature and the Specific Signal-To-Noise Properties of Each Measure." *Brain Imaging and Behavior* 15: 389–400. https://doi.org/10.1007/s11682-020-00266-x.

Deng, S., C. G. Franklin, M. O'Boyle, et al. 2022. "Hemodynamic and Metabolic Correspondence of Resting-State Voxel-Based Physiological Metrics in Healthy Adults." *NeuroImage* 250: 118923. https://doi.org/10.1016/j.neuroimage.2022.118923.

Di Martino, A., D. O'Connor, B. Chen, et al. 2017. "Enhancing Studies of the Connectome in Autism Using the Autism Brain Imaging Data Exchange II." *Scientific Data* 4, no. 1: 1–15. https://doi.org/10.1038/sdata.2017.10.

Di Martino, A., C. G. Yan, Q. Li, et al. 2013. "The Autism Brain Imaging Data Exchange: Towards a Large-Scale Evaluation of the Intrinsic Brain Architecture in Autism." *Molecular Psychiatry* 19, no. 6: 659–667. https://doi.org/10.1038/mp.2013.78.

Eklund, A., T. E. Nichols, and H. Knutsson. 2016. "Cluster Failure: Why fMRI Inferences for Spatial Extent Have Inflated False-Positive Rates." *Proceedings of the National Academy of Sciences of the United States of America* 113, no. 28: 7900–7905. https://doi.org/10.1073/pnas.1602413113.

Feis, R. A., M. J. R. J. Bouts, E. G. P. Dopper, et al. 2019. "Multimodal MRI of Grey Matter, White Matter, and Functional Connectivity in Cognitively Healthy Mutation Carriers at Risk for Frontotemporal Dementia and Alzheimer's Disease." *BMC Neurology* 19: 343. https://doi.org/10.1186/s12883-019-1567-0.

Ferguson, B. R., and W.-J. Gao. 2015. "Development of Thalamocortical Connections Between the Mediodorsal Thalamus and the Prefrontal Cortex and Its Implication in Cognition." *Frontiers in Human Neuroscience* 8: 1027. https://doi.org/10.3389/fnhum.2014.01027.

Figueroa-Jiménez, M. D., C. Cañete-Massé, E. Gudayol-Ferre, G. B. Gallardo-Moreno, M. Peró-Cebollero, and J. Guàrdia-Olmos. 2024. "Functional Brain Hubs Are Related to Age: A Primer Study With Rs-fMRI." *International Journal of Clinical and Health Psychology* 24: 100517. https://doi.org/10.1016/j.ijchp.2024.100517.

Fortin, J. P., N. Cullen, Y. I. Sheline, et al. 2018. "Harmonization of Cortical Thickness Measurements Across Scanners and Sites." *NeuroImage* 167: 104–120. https://doi.org/10.1016/J.NEUROIMAGE.2017.11.024.

Fortin, J. P., D. Parker, B. Tunç, et al. 2017. "Harmonization of Multi-Site Diffusion Tensor Imaging Data." *NeuroImage* 161: 149–170. https://doi.org/10.1016/J.NEUROIMAGE.2017.08.047.

Fox, M. D., and M. E. Raichle. 2007. "Spontaneous Fluctuations in Brain Activity Observed With Functional Magnetic Resonance Imaging." *Nature Reviews Neuroscience* 8: 700–711. https://doi.org/10.1038/nrn2201.

Friston, K. J., S. Williams, R. Howard, R. S. J. Frackowiak, and R. Turner. 1996. "Movement-Related Effects in fMRI Time-Series." *Magnetic Resonance in Medicine* 35, no. 3: 346–355. https://doi.org/10.1002/MRM.1910350312.

Grill-Spector, K., K. S. Weiner, J. Gomez, A. Stigliani, and V. S. Natu. 2018. "The Functional Neuroanatomy of Face Perception: From Brain Measurements to Deep Neural Networks." *Interface Focus* 8: 20180013. https://doi.org/10.1098/rsfs.2018.0013.

Guo, X., X. Duan, H. Chen, et al. 2019. "Altered Inter- and Intrahemispheric Functional Connectivity Dynamics in Autistic Children." *Human Brain Mapping* 41: 419–428. https://doi.org/10.1002/hbm.24812.

Hafkemeijer, A., I. Altmann-Schneider, A. M. Oleksik, et al. 2013. "Increased Functional Connectivity and Brain Atrophy in Elderly With Subjective Memory Complaints." *Brain Connectivity* 3, no. 4: 353–362. https://doi.org/10.1089/brain.2013.0144.

He, J., K. Kurita, T. Yoshida, K. Matsumoto, E. Shimizu, and Y. Hirano. 2024. "Comparisons of the Amplitude of Low-Frequency Fluctuation and Functional Connectivity in Major Depressive Disorder and Social Anxiety Disorder: A Resting-State fMRI Study." *Journal of Affective Disorders* 362: 425–436. https://doi.org/10.1016/j.jad.2024.07.020.

Hoffstaedter, F., C. Grefkes, C. Roski, S. Caspers, K. Zilles, and S. B. Eickhoff. 2015. "Age-Related Decrease of Functional Connectivity Additional to Gray Matter Atrophy in a Network for Movement Initiation." *Brain Structure and Function* 220: 999–1012. https://doi.org/10.1007/s00429-013-0696-2.

Huck, J., A. T. Jäger, U. Schneider, et al. 2023. "Modeling Venous Bias in Resting-State Functional MRI Metrics." *Human Brain Mapping* 44: 4938–4955. https://doi.org/10.1002/hbm.26431.

Içer, S. 2019. "Functional Connectivity Differences in Brain Networks From Childhood to Youth." *International Journal of Imaging Systems and Technology* 30, no. 1: 75–91. https://doi.org/10.1002/ima.22366.

Ingalhalikar, M., S. Shinde, A. Karmarkar, A. Rajan, D. Rangaprakash, and G. Deshpande. 2021. "Functional Connectivity-Based Prediction of Autism on Site harmonizedABIDE Dataset." *IEEE Transactions on Biomedical Engineering* 68, no. 12: 3628–3637. https://doi.org/10.1109/TBME.2021.3080259.

Jenkinson, M., P. Bannister, M. Brady, and S. Smith. 2002. "Improved Optimization for the Robust and Accurate Linear Registration and Motion Correction of Brain Images." *NeuroImage* 17, no. 2: 825–841. https://doi.org/10.1006/NIMG.2002.1132.

Johnson, W. E., C. Li, and A. Rabinovic. 2007. "Adjusting Batch Effects in Microarray Expression Data Using Empirical Bayes Methods." *Biostatistics* 8, no. 1: 118–127. https://doi.org/10.1093/BIOSTATISTICS/KXJ037.

Jolles, D. D., M. A. van Buchem, E. A. Crone, and S. A. Rombouts. 2011. "A Comprehensive Study of Whole-Brain Functional Connectivity in Children and Young Adults." *Cerebral Cortex* 21, no. 2: 385–391. https://doi.org/10.1093/cercor/bhq104.

Kim, T. H., E. Choi, H. Kim, et al. 2021. "The Association Between Hippocampal Volume and Level of Attention in Children and Adolescents." *Frontiers in Systems Neuroscience* 15: 671735. https://doi.org/10.3389/fnsys.2021.671735.

Langen, C. D., R. Muetzel, L. Blanken, et al. 2018. "Differential Patterns of Age-Related Cortical and Subcortical Functional Connectivity in 6-To-10 Year Old Children: A Connectome-Wide Association Study." *Brain and Behavior: A Cognitive Neuroscience Perspective* 8, no. 8: e01031. https://doi.org/10.1002/brb3.1031.

Li, C. L., Y. J. Deng, Y. H. He, Y. C. Zhai, and F. C. Jia. 2019. "The Development of Brain Functional Connectivity Networks Revealed by Resting-State Functional Magnetic Resonance Imaging." *Neural Regeneration Research* 14, no. 8: 1419–1429. https://doi.org/10.4103/1673-5374.253526.

Li, H., M. Han, S. Tang, and Y. Yang. 2024. "Dynamic and Static Brain Functional Abnormalities in Autism Patients at Different Developmental Stages." *Neuroreport* 36, no. 4: 202–210. https://doi.org/10.1097/WNR.0000000000002139.

Loh, M. K., and J. A. Ronsenkranz. 2022. "Shifts in Medial Orbitofrontal Cortex Activity From Adolescence to Adulthood." *Cerebral Cortex* 32: 528–539. https://doi.org/10.1093/cercor/bhab231.

Ma, Y., C. Zhang, D. Xiong, H. Zhang, and S. Ying. 2026. "Multi-Task Dynamic Graph Learning for Brain Disorder Identification With Functional MRI." *Pattern Recognition* 170: 111922. https://doi.org/10.1016/j.patcog.2025.111922.

Maldjian, J. A., P. J. Laurienti, and J. H. Burdette. 2004. "Precentral Gyrus Discrepancy in Electronic Versions of the Talairach Atlas." *NeuroImage* 21, no. 1: 450–455. https://doi.org/10.1016/J.NEUROIMAGE.2003.09.032.

Maldjian, J. A., P. J. Laurienti, R. A. Kraft, and J. H. Burdette. 2003. "An Automated Method for Neuroanatomic and Cytoarchitectonic Atlas-Based Interrogation of fMRI Data Sets." *NeuroImage* 19, no. 3: 1233–1239. https://doi.org/10.1016/S1053-8119(03)00169-1.

Marek, S., K. Hwang, W. Foran, M. N. Hallquist, and B. Luna. 2015. "The Contribution of Network Organization and Integration to the Development of Cognitive Control." *PLoS Biology* 13, no. 12: e1002328. https://doi.org/10.1371/journal.pbio.1002328.

Mastrangelo, S., L. Peruzzi, A. Guido, et al. 2024. "The Role of the Cerebellum in Advanced Cognitive Processes in Children." *Biomedicine* 12, no. 8: 1707. https://doi.org/10.3390/biomedicines12081707.

Mateu-Estivill, R., A. Adan, S. Grau, et al. 2024. "Alterations in Functional Brain Connectivity Associated With Developmental Dyscalculia." *Journal of Neuroimaging* 34: 694–703. https://doi.org/10.1111/jon.13236.

Mills, K. L., K. D. Siegmund, C. K. Tamnes, et al. 2021. "Inter-Individual Variability in Structural Brain Development From Late Childhood to Young Adulthood." *NeuroImage* 242: 118450. https://doi.org/10.1016/j.neuroimage.2021.118450.

Montalà-Flaquer, M., C. Cañete-Massé, L. Vaqué-Alcázar, D. Bartrés-Faz, M. Peró-Cebollero, and J. Guàrdia-Olmos. 2023. "Spontaneous Brain Activity in Healthy Aging: An Overview Through Fluctuations and Regional Homogeneity." *Frontiers in Aging Neuroscience* 14: 1002811. https://doi.org/10.3389/fnagi.2022.1002811.

Ouyang, M., M. T. Whitehead, S. Mohapatra, T. Zhu, and H. Huang. 2024. "Machine-Learning Based Prediction of Future Outcome Using Multimodal MRI During Early Childhood." *Seminars in Fetal and Neonatal Medicine* 29, no. 2: 101561. https://doi.org/10.1016/j.siny.2024.101561.

Porcu, M., M. Wintermark, J. S. Suri, and L. Saba. 2019. "The Influence of the Volumetric Composition of the Intracranial Space on Neural Activity in Healthy Subjects: A Resting-State Functional Magnetic Resonance Study." *European Journal of Neuroscience* 51, no. 9: 1944–1961. https://publons.com/publon/10.1111/ejn.14627.

Razi, A., and K. J. Friston. 2016. "The Connected Brain Causality, Models, and Intrinsic Dynamics." *IEEE Signal Processing Magazine* 33, no. 3: 14–35. https://doi.org/10.1109/Msp.2015.2482121.

Ruan, L., G. Chen, M. Yao, et al. 2024. "Brain Functional Gradient and Structure Features in Adolescent and Adult Autism Spectrum Disorders." *Human Brain Mapping* 45, no. 11: e26792. https://doi.org/10.1002/hbm.26792.

Sala-Llonch, R., D. Bartrés-Faz, and C. Junqué. 2015. "Reorganization of Brain Networks in Aging: A Review of Functional Connectivity Studies." *Frontiers in Psychology* 6: 136321. https://doi.org/10.3389/fpsyg.2015.00663.

Sanders, A. F. P., A. P. Harms, S. Kandala, et al. 2023. "Age-Related Differences in Resting-State Functional Connectivity From Childhood to Adolescence." *Cerebral Cortex* 33: 6928–6942. https://doi.org/10.1093/cercor/bhad011.

Sato, J. R., G. A. Salum, A. Gadelha, et al. 2015. "Decreased Centrality of Subcortical Regions During the Transition to Adolescence: A Functional Connectivity Study." *NeuroImage* 104: 44–51. https://doi.org/10.1016/j.neuroimage.2014.09.063.

Soman, S. M., N. Vijayakumar, P. Thomson, G. Ball, C. Hyde, and T. J. Silk. 2023. "Functional and Structural Brain Network Development in Children With Attention Deficit Hyperactivity Disorder." *Human Brain Mapping* 44, no. 8: 3394–3409. https://doi.org/10.1002/hbm.26288.

Stoodley, C. J., and J. D. Schmahmann. 2009. "Functional Topography in the Human Cerebellum: A Meta-Analysis of Neuroimaging Studies." *NeuroImage* 44, no. 2: 489–501. https://doi.org/10.1016/j.neuroimage.2008.08.039.

Supekar, K., L. Q. Uddin, K. Prater, H. Amin, M. D. Greicius, and V. Menon. 2010. "Development of Functional and Structural Connectivity Within the Default Mode Network in Young Children." *NeuroImage* 52, no. 1: 290–301. https://doi.org/10.1016/j.neuroimage.2010.04.009.

Tapia-Medina, M. G., R. Cosío-Guirado, M. Peró-Cebollero, C. C. Massé, E. R. Villuendas-González, and J. Guàrdia-Olmos. 2025. "The Clinical Relevance of Healthy Neurodevelopmental Connectivity in Childhood and Adolescence: A Meta-Analysis of Resting-State fMRI." *Frontiers in Neuroscience* 19: 1576932. https://doi.org/10.3389/fnins.2025.1576932.

Tarchi, L., S. Damiani, P. T. Vittori, et al. 2023. "Progressive Voxel-Wise Homotopic Connectivity From Childhood to Adulthood: Age-Related Functional Asymmetry in Resting-State Functionalmagnetic Resonance Imaging." *Developmental Psychobiology* 65, no. 2: e22366. https://doi.org/10.1002/dev.22366.

Tian, Y., G. Xu, J. Zhang, K. Chen, and S. Liu. 2023. "Nodal Properties of the Resting-State Brain Functional Network in Childhood and Adolescence." *Journal of Neuroimaging* 33: 1015–1023. https://doi.org/10.1111/jon.13155.

Tommasin, S., D. Mascali, T. Gili, et al. 2017. "Task-Related Modulations of BOLD Low-Frequency Fluctuations Within the Default Mode Network." *Frontiers in Physics* 5, no. 31. https://doi.org/10.3389/fphy.2017.00031.

Tzourio-Mazoyer, N., B. Landeau, D. Papathanassiou, et al. 2002. "Automated Anatomical Labeling of Activations in SPM Using a Macroscopic Anatomical Parcellation of the MNI MRI Single-Subject Brain." *NeuroImage* 15, no. 1: 273–289. https://doi.org/10.1006/nimg.2001.0978.

Uddin, L. Q., F. X. Castellanos, and V. Menon. 2025. "Resting State Functional Brain Connectivity in Child and Adolescent Psychiatry: Where Are We Now?" *Neuropsychopharmacology* 50: 196–200. https://doi.org/10.1038/s41386-024-01888-1.

Wainberg, M., G. R. Jacobs, A. N. Voineskos, and S. J. Tripathy. 2022. "Neurobiological, Familial and Genetic Risk Factors for Dimensional Psychopathology in the Adolescent Brain Cognitive Development Study." *Molecular Psychiatry* 27, no. 6: 2731–2741. https://doi.org/10.1038/S41380-022-01522-W.

Wang, S., L. Yue, C. Cui, et al. 2019. "Top-Down Control of the Medial Orbitofrontal Cortex to Nucleus Accumbens Core Pathway in Decisional Impulsivity." *Brain Structure and Function* 224: 2437–2452. https://doi.org/10.1007/s00429-019-01913-w.

Wang, S., Y. Zhao, L. Zhang, et al. 2019. "Stress and the Brain: Perceived Stress Mediates the Impact of the Superior Frontal Gyrus Spontaneous Activity on Depressive Symptoms in Late Adolescence." *Human Brain Mapping* 40: 4982–4993. https://doi.org/10.1002/hbm.24752.

Wang, Y., L. Wan, W. Yang, et al. 2025. "Differential Abnormality in Regional Brain Spontaneous Activity and Functional Connectivity in Patients of Non-Acute Subcortical Stroke With Versus Without Global Cognitive Functional Impairment." *Brain and Behavior: A Cognitive Neuroscience Perspective* 15: e70356. https://doi.org/10.1002/brb3.70356.

Wang, Y. W., H. L. Wang, and C. G. Yan. 2024. "DPABI Harmonization: A Toolbox for Harmonizing Multi-Site Brain Imaging for Big-Data Era." *Imaging Neuroscience* 2: 1–17. https://doi.org/10.1162/imag_a_00388.

Welvaert, M., and Y. Rosseel. 2014. "A Review of fMRI Simulation Studies." *PLoS One* 9, no. 7: e101953. https://doi.org/10.1371/journal.pone.0101953.

Whitfield-Gabrieli, S., C. Wendelken, A. Nieto-Castañón, et al. 2020. "Association of Intrinsic Brain Architecture With Changes in Attentional and Mood Symptoms During Development." *JAMA Psychiatry* 77, no. 4: 378–386. https://doi.org/10.1001/jamapsychiatry.2019.4208.

Xu, W., F. Ying, Y. Luo, X. Y. Zhang, and Z. Li. 2021. "Cross-Sectional Exploration of Brain Functional Connectivity in the Triadic Development Model of Adolescents." *Brain Imaging and Behavior* 15: 1855–1867. https://doi.org/10.1007/s11682-020-00379-3.

Xu, Y., and Y. Zhang. 2023. "Abnormal Voxel-Mirrored Homotopic Connectivity in Firstepisode, Drug-naïve Patients With Obsessive–Compulsive Disorder." *European Journal of Neuroscience* 58: 3531–3539. https://doi.org/10.1111/ejn.16117.

Yan, C. G., B. Cheung, C. Kelly, et al. 2013. "A Comprehensive Assessment of Regional Variation in the Impact of Head Micromovements on Functional Connectomics." *NeuroImage* 76: 183–201. https://doi.org/10.1016/J.NEUROIMAGE.2013.03.004.

Yan, C. G., X. Di Wang, X. N. Zuo, and Y. F. Zang. 2016. "DPABI: Data Processing & Analysis for (Resting-State) Brain Imaging." *Neuroinformatics* 14, no. 3: 339–351. https://doi.org/10.1007/S12021-016-9299-4.

Yan, C. G., and Y. F. Zang. 2010. "DPARSF: A MATLAB Toolbox for "Pipeline" Data Analysis of Resting-State fMRI." *Frontiers in Systems Neuroscience* 4: 13. https://doi.org/10.3389/fnsys.2010.00013.

Yang, H., X. Y. Long, Y. Yang, et al. 2007. "Amplitude of Low Frequency Fluctuation Within Visual Areas Revealed by Resting-State Functional MRI." *NeuroImage* 36: 144–152. https://doi.org/10.1016/j.neuroimage.2007.01.054.

Zang, Y., T. Jiang, Y. Lu, Y. He, and L. Tian. 2004. "Regional Homogeneity Approach to fMRI Data Analysis." *NeuroImage* 22: 394–400. https://doi.org/10.1016/j.neuroimage.2003.12.030.

Zhang, J., A. Kucyi, J. Raya, et al. 2021. "What Have We Really Learned From Functional Connectivity in Clinical Populations?" *NeuroImage* 242: 118466. https://doi.org/10.1016/j.neuroimage.2021.118466.

Zhou, J., G. Yingxue, B. Xuan, et al. 2018. "A Multi-Parameter Resting-State Functional Magnetic Resonance Imaging Study of Brain Intrinsic Activity in Attention Deficit Hyperactivity Disorder Children." *Journal of Biomedical Engineering* 35, no. 3: 415–420. https://doi.org/10.7507/1001-5515.201801001.

Zhu, J., Y. Zhang, B. Zhang, et al. 2019. "Abnormal Coupling Among Spontaneous Brain Activity Metrics and Cognitive Deficits in Major Depressive Disorder." *Journal of Affective Disorders* 252: 74–83. https://doi.org/10.1016/j.jad.2019.04.030.

Zhu, J., D. M. Zhu, Y. Qian, X. Li, and Y. Yu. 2018. "Altered Spatial and Temporal Concordance Among Intrinsic Brain Activity Measures in Schizophrenia." *Journal of Psychiatric Research* 106: 91–98. https://doi.org/10.1016/j.jpsychires.2018.09.015.

Zou, Q. H., C. Z. Zhu, Y. Yang, et al. 2008. "An Improved Approach to Detection of Amplitude of Low-Frequency Fluctuation (ALFF) for Resting-State fMRI: Fractional ALFF." *Journal of Neuroscience Methods* 172, no. 1: 137–141. https://doi.org/10.1016/j.jneumeth.2008.04.012.

Zuo, X. N., C. Kelly, A. Di Martino, et al. 2010. "Growing Together and Growing Apart: Regional and Sex Differences in the Lifespan Developmental Trajectories of Functional Homotopy." *Journal of Neuroscience* 30, no. 45: 15034. https://doi.org/10.1523/JNEUROSCI.2612-10.2010.

Supporting Information

Additional supporting information can be found online in the Supporting Information section. **Data S1:** Figures S1–S5.